Lecture 06

Fundamentals of Error Analysis and Radiometry

AST-B09 Observational Astronomy

Rogério Monteiro-Oliveira, Ph.D. (孟羅傑)

Goals of Lecture 06

This lecture establishes the statistical, instrumental, and physical frameworks required to quantify astronomical signals. We bridge the gap between the probabilistic nature of photon arrival, the electronic response of CCD detectors, and the fundamental physics of radiometric energy transfer. The primary objectives are to:

- Define the core probability distributions (Binomial, Poisson, Gaussian) that govern photon counting and the fundamental nature of astronomical measurement.
- Apply the general law of error propagation to differentiate between random and systematic errors, rigorously quantifying uncertainties in derived parameters like sky background and magnitudes.
- Deconstruct the CCD equation to map the conversion of incident photons to digital signals (ADUs) through quantum efficiency and gain, and derive the Signal-to-Noise Ratio (SNR) across various observing regimes.
- Formulate the principles of radiometry, linking specific intensity and flux density to distance, Kirchhoff's Laws, and intrinsic blackbody radiation.

Contents

1 The Fundamental Nature of Astronomical Measurement

Astrophysics occupies a uniquely challenging position among the empirical sciences: with extremely rare exceptions, we cannot interact with, manipulate, or isolate our subjects of study. We are exclusively passive receivers of a tenuous, degrading stream of information. Whether we are utilizing a modern Charge-Coupled Device (CCD) at the focal plane of an 8-meter telescope or a primitive photomultiplier tube, the fundamental observable remains the same: the arrival of individual, discrete packets of electromagnetic energy, *photons*.

Observation, therefore, is fundamentally an act of counting. However, modern observational techniques are not merely concerned with the mechanical operation of instruments to collect these counts. Rather, they represent the rigorous mathematical discipline of extracting an underlying physical truth from an inherent sea of noise. The raw signal we record on a detector is never the exact, unadulterated truth of the universe; it is a single statistical realization of a quantum mechanical process, heavily convoluted by the Earth's atmosphere (via extinction, scattering, and turbulence) and the instrument's own thermal and electronic signatures.

Consequently, in the physical sciences, a measurement devoid of a rigorously quantified uncertainty is scientifically meaningless. The robust characterization of the error (understanding the probability distribution that governs it, its physical origins, and how it propagates through our reduction algorithms) is as critical as the measurement itself. The uncertainty dictates the statistical significance of a new discovery, constrains the viability of theoretical models, and ultimately defines the boundaries of our cosmic knowledge.

2 Probability Functions in Astronomy

In observational astronomy, we measure the number of events (photon arrivals) that occur within a specific interval of time (the exposure time). Because the emission of photons by an astrophysical source and their subsequent arrival at our detector are independent, random events, they are strictly governed by specific probability distribution functions (PDFs).

2.1 The Binomial Distribution

At the most fundamental quantum level, the detection of light can be modeled as a series of independent success/failure experiments, governed by the binomial distribution. Suppose we have n independent trials, each with a probability of success p and a probability of failure $(1-p)$. The probability of observing exactly x successes is given by:

$$P(x;n,p) = \frac{n!}{x!(n-x)!}p^x(1-p)^{n-x} \tag{1}$$

For a binomial distribution, the expectation value (mean) is $\mu = np$, and the variance is $\sigma^2 = np(1-p)$.

In observational astronomy, the binomial distribution accurately describes processes involving fractional efficiencies. For example, consider the Quantum Efficiency (QE) of a CCD. If exactly n photons strike a pixel, and each photon has a probability p (the QE) of undergoing the photoelectric effect to liberate an electron, the number of actually recorded photoelectrons follows a binomial distribution.

Crucially, the binomial distribution provides the mathematical origin of the Poisson distribution. Consider a star emitting an unfathomably large number of photons ($n \to \infty$). The probability p that any specific emitted photon travels across the galaxy, survives interstellar extinction, penetrates the Earth's atmosphere, and happens to hit our specific telescope mirror is infinitesimally small ($p \to 0$). However, the product of these two extremes yields a finite, measurable rate of photon arrivals ($\mu = np$). In this extreme limit, the binomial distribution simplifies perfectly into the Poisson distribution.

2.2 The Poisson Distribution

The fundamental distribution governing astronomical counting statistics is the Poisson distribution. As derived from the limiting case of the binomial distribution, it describes the probability of observing exactly x events in a fixed interval of time, given that these events occur with a known constant mean rate and independently of the time since the last event.

If the expected true mean number of photons arriving in a given time interval is μ, the probability of actually measuring exactly x photons is given by:

$$P(x;\mu) = \frac{\mu^x e^{-\mu}}{x!} \tag{2}$$

where x is a non-negative integer ($x = 0, 1, 2, \ldots$).

A remarkable and highly convenient property of the Poisson distribution is the mathematical relationship between its mean (expected value) and its variance (σ^2). The expectation value is defined as:

$$E[x] = \sum_{x=0}^{\infty} xP(x;\mu) = \mu \tag{3}$$

The variance is defined as the expectation value of the squared deviation from the mean:

$$\sigma^2 = E[(x-\mu)^2] = \sum_{x=0}^{\infty}(x-\mu)^2 P(x;\mu) = \mu \tag{4}$$

Thus, for a Poisson process, the variance is exactly equal to the mean. The standard deviation, which represents the fundamental "noise" or uncertainty of our measurement, is simply the square root of the mean:

$$\sigma = \sqrt{\mu} \approx \sqrt{N} \tag{5}$$

where N is the actual number of photons counted. This gives rise to the fundamental limit of astronomical observation: **Poisson noise** (or shot noise). If you collect N photons from a star, your intrinsic uncertainty is $\sqrt{N}$. The fractional error is $\sqrt{N}/N = 1/\sqrt{N}$. Therefore, to improve your measurement precision by a factor of 2, you must collect 4 times as many photons.

2.3 The Gaussian (Normal) Distribution

While the Poisson distribution is exact for discrete counting, it becomes computationally inconvenient for large values of N (calculating $N!$ for $N = 10^6$ photons is non-trivial). Fortunately, due to the Central Limit Theorem, as $\mu \to \infty$, the discrete Poisson distribution asymptotically approaches the continuous Gaussian (or Normal) distribution.

In practice, for $N \gtrsim 30$, the Poisson distribution is excellently approximated by a Gaussian with mean μ and standard deviation $\sigma = \sqrt{\mu}$, as visually demonstrated in Figure 1:

$$P(x; \mu, \sigma) = \frac{1}{\sigma\sqrt{2\pi}} \exp\left[-\frac{1}{2}\left(\frac{x-\mu}{\sigma}\right)^2\right] \tag{6}$$

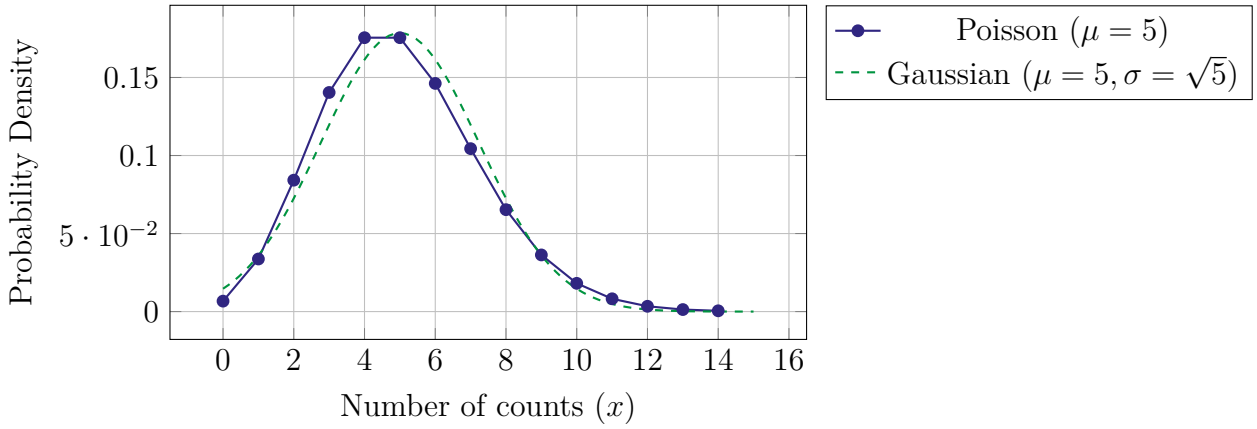

Figure 1: Comparison of the discrete Poisson distribution and the continuous Gaussian approximation for a low count rate ($\mu = 5$). As μ increases, the asymmetry of the Poisson distribution vanishes, and the two curves become indistinguishable.

The Gaussian distribution is symmetric and describes not only large photon counts but also the distribution of read noise in the CCD amplifier. When we discuss "confidence intervals" in astronomy, we are relying on Gaussian integrals. As illustrated in Figure 2, a result quoted as $x \pm 1\sigma$ implies a 68.3% probability that the true value lies within that range. A 3σ detection implies 99.7% confidence, and a 5σ detection (the gold standard for new discoveries) implies 99.99994% confidence.

3 Error Theory and Propagation

Measurements in astronomy are rarely utilized in isolation as raw detector counts. To extract meaningful physical quantities, we must subject our raw data to a rigorous pipeline of mathematical transformations: we subtract sky background from stellar fluxes, divide fluxes by calibration flat-fields, and convert linear counts into logarithmic magnitudes. Each mathematical operation inevitably propagates the initial quantum uncertainties into the final derived parameter.

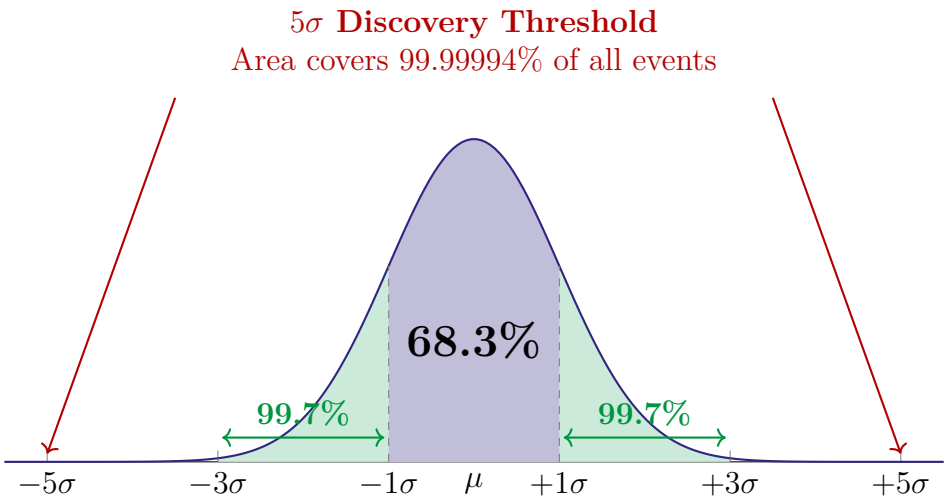

Figure 2: The Gaussian (Normal) probability density function. The central shaded region represents the 1σ confidence interval (containing 68.3% of the total area). The wider region marks the 3σ interval (99.7%). In astronomy, a 5σ deviation represents a probability of a false positive so small (1 in 3.5 million) that it is the standard required to claim a new discovery.

3.1 Random versus Systematic Errors

Before developing the mathematical machinery of error propagation, it is crucial to formally distinguish between the two fundamental classes of experimental uncertainty: random errors and systematic errors. This fundamental distinction (often framed as the difference between precision and accuracy) is visually encapsulated by the classic target analogy shown in Figure 3.

Random errors arise from inherently unpredictable, statistical fluctuations in the measurement process. In astronomy, the quintessential random error is the Poisson noise associated with discrete photon counting. Because these errors randomly scatter your measurements around the true value, they strictly dictate the *precision* of a measurement. Random errors can be rigorously quantified using probability density functions and can be fundamentally reduced by integrating for longer exposure times (recall the fractional error shrinks as $1/\sqrt{N}$). The mathematical error propagation equations developed in the following sections apply exclusively to random errors.

Systematic errors, by contrast, are deterministic inaccuracies that consistently shift measurements in a specific direction, fundamentally compromising the *accuracy* of the final result. They arise from physical flaws or oversights within the observational setup. Common astronomical examples include:

- **Equipment malfunctioning:** A non-linear CCD amplifier, poor telescope tracking that smears the Point Spread Function (PSF), or a malfunctioning shutter causing timing errors.
- **Incorrect measuring processes:** Dividing a science image by a flat-field taken

at a different focus setting, or failing to properly subtract the dark current.

- **Failures in measurement methodology:** Using a single aperture size for all stars regardless of seeing conditions, or neglecting to apply color-term corrections when calculating atmospheric extinction.

Critically, systematic errors *cannot* be reduced simply by collecting more photons or averaging multiple exposures. They do not obey counting statistics and must instead be meticulously identified, physically modeled, and calibrated out of the data.

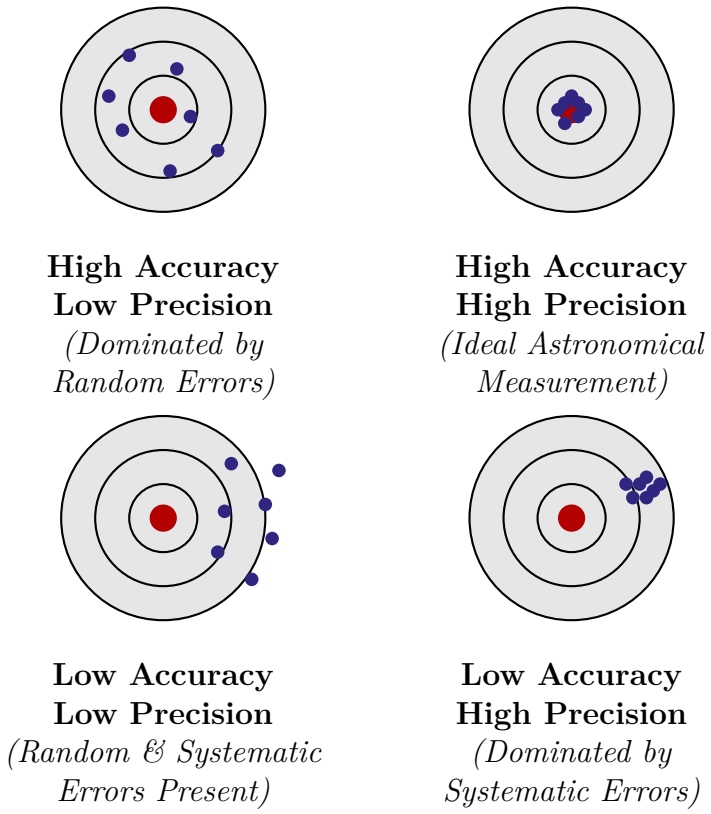

Figure 3: The classic target analogy illustrating the difference between random and systematic uncertainties. The true physical value is the red bullseye. Random errors scatter the measurements widely (reducing precision). Systematic errors physically shift the grouping away from the true value (reducing accuracy). Increasing integration time only tightens the grouping; it cannot fix a systematic offset.

3.2 The General Law of Error Propagation

Suppose we wish to calculate a derived physical quantity f, which is a continuous and differentiable function of n directly measured variables $x_1, x_2, \ldots, x_n$:

$$f = f(x_1, x_2, \ldots, x_n) \tag{7}$$

If the uncertainties (standard deviations σ_{x_i}) on these variables are small relative to the measured values themselves, we can approximate the variance of f by expanding it in a

first-order multivariate Taylor series. Squaring this expansion and taking the expectation value yields the exact, general formula for the propagation of variance:

$$\sigma_f^2 = \sum_{i=1}^{n} \left(\frac{\partial f}{\partial x_i} \right)^2 \sigma_{x_i}^2 + 2 \sum_{i=1}^{n-1} \sum_{j=i+1}^{n} \left(\frac{\partial f}{\partial x_i} \right) \left(\frac{\partial f}{\partial x_j} \right) \sigma_{x_i x_j} \tag{8}$$

The second sum introduces the *covariance* term, $\sigma_{x_i x_j}$, which dictates how two variables fluctuate together. In basic photometry, we often assume that our measured variables (like source photons and dark current) are fundamentally independent statistical processes, meaning the covariance terms vanish ($\sigma_{x_i x_j} = 0$). Under this assumption of mutual independence, the equation collapses into the standard form:

$$\sigma_f^2 = \sum_{i=1}^{n} \left(\frac{\partial f}{\partial x_i} \right)^2 \sigma_{x_i}^2 \tag{9}$$

A Critical Caveat: While Eq. 9 is ubiquitous, the researcher must exercise caution. If your reduction pipeline introduces correlations, such as interpolating and resampling pixels to align images, the variables are no longer independent. Ignoring the covariance term in such cases will artificially underestimate your photometric error.

Let us examine two ubiquitous applications of this law in observational astronomy.

3.3 Example 1: Subtracting Sky Background

In aperture photometry, we measure the total counts in a circular aperture containing a star (N_{total}). However, this aperture also contains flux from the sky background. We estimate the total sky background within that aperture (N_{sky}) using an adjacent region of the image. The true source flux N_* is:

$$N_* = N_{total} - N_{sky} \tag{10}$$

Applying the simplified propagation of errors (assuming the source and sky emissions are independent Poisson processes):

$$\sigma_{N_*}^2 = \left(\frac{\partial N_*}{\partial N_{total}} \right)^2 \sigma_{N_{total}}^2 + \left(\frac{\partial N_*}{\partial N_{sky}} \right)^2 \sigma_{N_{sky}}^2 \tag{11}$$

Since the partial derivatives are 1 and -1 (which squares to 1), we find:

$$\sigma_{N_*}^2 = \sigma_{N_{total}}^2 + \sigma_{N_{sky}}^2 \tag{12}$$

Because counting statistics fundamentally follow a Poisson distribution, their variances are equal to their mean expected values: $\sigma_{N_{total}}^2 = N_{total}$ and $\sigma_{N_{sky}}^2 = N_{sky}$. Therefore:

$$\sigma_{N_*} = \sqrt{N_{total} + N_{sky}} \tag{13}$$

Crucial Insight: Even though we physically *subtract* the signal of the sky, we must mathematically *add* its variance. Background light always inflates the noise of our measurement. Furthermore, in rigorous CCD photometry, N_{sky} is an estimate derived from an annulus of finite area. The uncertainty $\sigma_{N_{sky}}^2$ must actually include both the Poisson noise of the sky itself *and* the statistical uncertainty of the mean sky value computed from that annulus.

3.4 Example 2: Error on a Magnitude

As we will define formally in L07, the apparent magnitude m is related to the flux F by $m = -2.5\log_{10}(F) + C$. Using the change of base rule $\log_{10}(F) = \ln(F)/\ln(10)$, we write:

$$m = -\frac{2.5}{\ln(10)}\ln(F) + C \approx -1.0857\ln(F) + C \tag{14}$$

Applying error propagation to find the photometric uncertainty in magnitude (σ_m) given a known uncertainty in flux (σ_F):

$$\sigma_m = \left|\frac{\partial m}{\partial F}\right|\sigma_F = \left|-1.0857\frac{1}{F}\right|\sigma_F = 1.0857\left(\frac{\sigma_F}{F}\right) \tag{15}$$

The term (σ_F/F) is the inverse of the Signal-to-Noise Ratio (SNR). Therefore, the error in magnitude is linearly proportional to the inverse of the SNR:

$$\sigma_m \approx \frac{1.0857}{\mathrm{SNR}} \tag{16}$$

An SNR of 100 yields a highly precise photometric error of roughly 0.01 magnitudes.

The Low-SNR Breakdown: It is paramount to recognize that this equation is an approximation derived from a first-order Taylor expansion, which inherently assumes that the error is small ($\sigma_F \ll F$). For faint sources ($\mathrm{SNR} \lesssim 3$), this approximation catastrophically fails. Because the magnitude scale is logarithmic, a positive flux fluctuation $+1\sigma_F$ yields a much smaller change in magnitude than a negative flux fluctuation $-1\sigma_F$. Consequently, at low signal-to-noise, magnitude errors become highly asymmetric, and quoting a symmetric $m \pm \sigma_m$ loses its statistical validity. In extreme cases where background subtraction yields a mathematically negative flux, the logarithm becomes undefined, necessitating the use of alternative metrics like the asinh magnitude system (Lupton magnitudes) used by the Sloan Digital Sky Survey.

4 The CCD Equation and the Astronomical Signal

The precision of astronomical photometry is fundamentally dictated by the Signal-to-Noise Ratio (SNR). In Astrostatistics, a standard threshold is that an $\mathrm{SNR} \geq 5$ constitutes a statistically firm detection. To accurately quantify this statistical error on a target's flux, we must understand the physical realities of the detector.

The modern workhorse of optical and near-infrared astronomy is the CCD. When photons hit the silicon lattice of a CCD, they liberate electrons via the photoelectric effect. The total measured signal is simply the number of photoelectrons generated by the astrophysical source, N_*. However, the total noise is an amalgamation of several distinct physical and electronic processes.

4.1 From Photons to Electrons: Quantum Efficiency

The initial stage of signal detection involves converting incident astrophysical photons into countable charge carriers. However, no detector is perfectly efficient. The **Quantum**

Efficiency (QE, often denoted mathematically as η) is the probability that a single incident photon will successfully liberate a photoelectron in the silicon lattice.

If a target delivers P_* photons to the telescope focal plane, the actual number of generated photoelectrons N_* is:

$$N_* = \eta P_* \tag{17}$$

QE is a strongly wavelength-dependent property ($\eta = \eta(\lambda)$). Modern back-illuminated CCDs can achieve peak quantum efficiencies exceeding 90% at visible wavelengths, drastically outperforming historical photographic plates.

It is crucial to note that the Poisson statistics dictating our source noise are governed by the number of *detected* electrons (N_*), not the raw number of incident photons (P_*). For our standard noise model, we will abstract the QE directly into the electron counts (N_*, N_S, N_D).

4.2 From Electrons to ADUs: The Role of Gain

Before detailing the noise sources, we must address the most common pitfall in observational photometry. A CCD does not output "electrons". The analog-to-digital converter (ADC) outputs arbitrary digital counts, often called Analog-to-Digital Units (ADUs) or simply Data Numbers (DN).

Because Poisson statistics fundamentally govern the discrete quantum counting of *physical events*, **you cannot apply Poisson statistics to ADUs**. You must first convert your digital image back into physical photoelectrons using the amplifier's **Gain** (g), defined in units of e^-/ADU:

$$N_{electrons} = g \times N_{ADU} \tag{18}$$

Every equation derived hereafter strictly assumes that all quantities have been converted into physical electrons.

4.3 Sources of Noise in a CCD

Because counting photons is a quantum mechanical process, it is governed by **Poisson statistics**, where the variance (σ^2) equals the mean number of expected events (μ). To construct our noise model, let us assume we measure a target star using a circular photometric aperture spanning n_{pix} pixels. The total noise is the quadrature sum of four independent sources, visually summarized in Figure 4:

1. **Source Photon Noise (σ_*):** The intrinsic Poisson variation in the arrival rate of photons from the target star. If the star generates N_* electrons, the variance is $\sigma_*^2 = N_*$.
2. **Sky Background Noise (σ_S):** The night sky naturally glows due to atmospheric airglow, scattered starlight, and moonlight. If the background contributes N_S electrons per pixel, the variance from the sky photons within our aperture is $n_{pix}N_S$.
3. **Dark Current Noise (σ_D):** Thermal energy in the silicon lattice spontaneously excites electrons into the conduction band, even in complete darkness. The rate

of dark current generation I_D (in e^-/pix/sec) is highly temperature-dependent, following the thermodynamic relationship:

$$I_D \propto T^{3/2} \exp\left(-\frac{E_g}{2k_B T}\right) \tag{19}$$

To suppress this thermal noise, astronomical CCDs are cryogenically cooled. Modern chips also utilize **Multi-Pinned Phase (MPP)** operation. By driving all clock gates into negative inversion during integration, MPP fills surface traps with holes, suppressing surface-generated dark current. If the remaining dark current yields N_D electrons per pixel, the variance in the aperture is $n_{pix} N_D$.

4. **Readout Noise (σ_R):** When the accumulated charge is shifted across the CCD and measured by the output amplifier, additive electronic noise is introduced. This noise is Gaussian, not Poissonian, and its root-mean-square value per pixel is σ_R (given in e^-/pixel). The total variance added per pixel is σ_R^2, so the total variance in the aperture is $n_{pix}\sigma_R^2$.

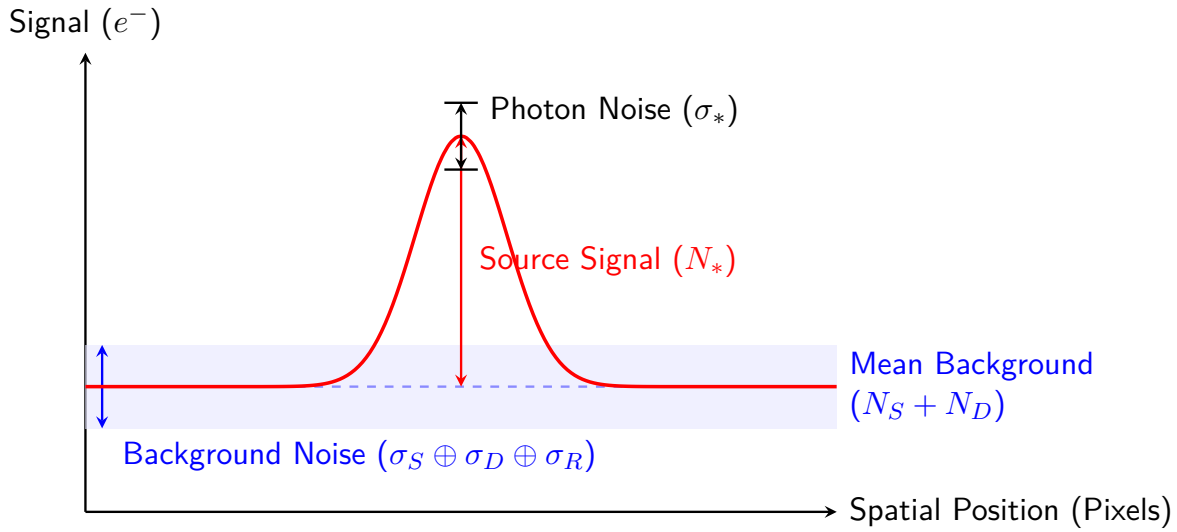

Figure 4: Visual representation of the Signal-to-Noise Ratio (SNR) components. The true source signal (N_*) must overcome both its intrinsic photon shot noise (σ_*) at the peak, and the underlying floor of background noise, which consists of sky glow, thermal dark current, and electronic readout noise.

Advanced Consideration: The Sky Estimation Penalty. In rigorous photometry, the sky background N_S is not perfectly known; it is an average value calculated from a background annulus of n_{sky} pixels. Because this mean value has its own statistical uncertainty ($\sigma^2_{mean} = N_S/n_{sky}$), subtracting the sky introduces an extra variance penalty. The true sky variance term is therefore $n_{pix} N_S \left(1 + \frac{n_{pix}}{n_{sky}}\right)$.

4.4 Deriving the Signal-to-Noise Ratio (SNR)

Because these noise sources are independent random processes, their variances add in quadrature. Ignoring the small sky-estimation penalty for simplicity, the Signal-to-Noise

Ratio (SNR) is the ratio of the true signal (N_*) to the total root-mean-square noise (σ_{total}):

$$\mathrm{SNR} = \frac{N_*}{\sqrt{N_* + n_{pix}(N_S + N_D + \sigma_R^2)}} \tag{20}$$

Equation 20 is known as the **CCD Equation**. It is arguably the most important equation in observational astronomy. It dictates exposure times, guides telescope design, and determines the ultimate feasibility of an observing program.

4.5 Limiting Regimes and Time Dependence

To build physical intuition, it is highly instructive to rewrite the CCD equation in terms of rates and integration time (t). Let R_*, R_S, and R_D be the rates of source electrons, sky electrons, and dark electrons per second, respectively. The signal is $N_* = R_* t$. Notice that while photon and dark counts grow continuously with t, the read noise (σ_R) is a fixed penalty paid exactly once per exposure.

We examine the CCD equation under three extreme regimes, visually summarized in Figure 5:

1. Source-Limited Regime (High SNR): If the star is very bright, $R_* t \gg n_{pix}(R_S t + R_D t + \sigma_R^2)$. The denominator is dominated by the photon noise of the star itself:

$$\mathrm{SNR} \approx \frac{R_* t}{\sqrt{R_* t}} = \sqrt{R_* t} \propto \sqrt{t} \tag{21}$$

Here, the measurement is limited purely by fundamental quantum statistics. SNR increases as the square root of integration time.

2. Background-Limited Regime (BLIP): If the star is faint but the sky is bright (e.g., broad-band optical imaging), the noise floor is dominated entirely by the Poisson noise of the glowing sky:

$$\mathrm{SNR} \approx \frac{R_* t}{\sqrt{n_{pix} R_S t}} = \frac{R_*}{\sqrt{n_{pix} R_S}} \sqrt{t} \propto \sqrt{t} \tag{22}$$

In this Background-Limited Performance (BLIP) regime, SNR still increases as $\sqrt{t}$. Because read noise is negligible compared to the sky glow, the observer can freely split long exposures into many shorter ones without suffering an SNR penalty.

3. Read-Noise-Limited Regime: For very faint targets requiring short exposures (or high-dispersion spectroscopy where the sky background per pixel is minimal), the fixed electronic read noise dominates the variance:

$$\mathrm{SNR} \approx \frac{R_* t}{\sqrt{n_{pix} \sigma_R^2}} = \left(\frac{R_*}{\sigma_R \sqrt{n_{pix}}} \right) t \propto t \tag{23}$$

Crucial Insight: In the read-noise limited regime, the SNR scales **linearly** with time, not as the square root! Taking one long 60-minute exposure will yield a drastically better SNR than co-adding sixty 1-minute exposures, because the latter forces you to pay the fixed read-noise penalty 60 separate times.

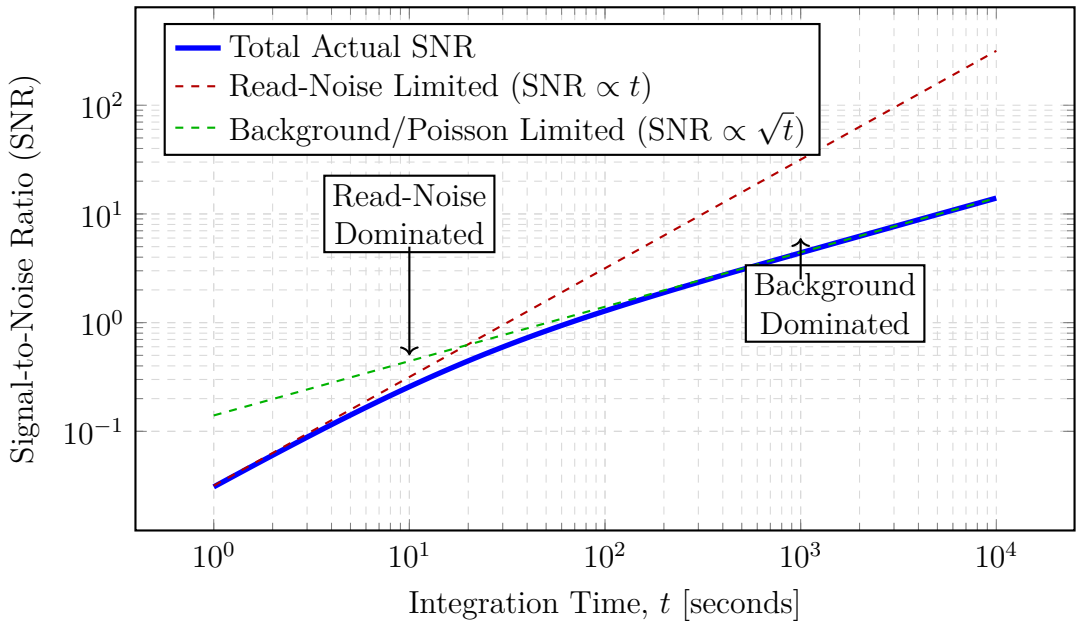

Figure 5: The time evolution of the Signal-to-Noise Ratio (SNR) for a faint source. For short integration times, the fixed electronic read-noise dominates the variance, and the SNR grows linearly with time (slope = 1 on a log-log plot). As the exposure continues, the accumulated Poisson variance of the sky background eventually surpasses the read noise. The system enters the Background-Limited (BLIP) regime, where SNR only grows as the square root of time (slope = 0.5).

5 Radiometry: Quantitative Measurements of Light

5.1 Flux Density, Specific Intensity, and Distance

Radiometry is fundamentally concerned with measuring the absolute physical energy arriving at a detector. At the macroscopic level, a radiation field is characterized by its **specific intensity**, I_ν. This is defined as the energy dE passing through a surface area dA, during a time interval dt, within a solid angle $d\Omega$, and across a frequency range $d\nu$:

$$I_\nu = \frac{dE}{dA\, dt\, d\Omega\, d\nu} \quad [\mathrm{W\ m^{-2}\ Hz^{-1}\ sr^{-1}}] \tag{24}$$

A practical question often arises in observational astronomy: *do we measure intensity or flux?*. A profound property of specific intensity is that **it is distance-independent** in a vacuum. To understand why, let us consider the optics of a telescope, as illustrated in Figure 6. Suppose the radiation emitted by an area element of the source, A_S, arrives at an area element of our detector, A_D (such as a single CCD pixel).

If our telescope has a focal length f, the solid angle ω subtended by the detector pixel is fixed by the instrument's geometry: $\omega = A_D/f^2$. By similar triangles, this must equal the solid angle subtended by the physical source area at a distance r:

$$\omega = \frac{A_D}{f^2} = \frac{A_S}{r^2} \tag{25}$$

What happens if the distance r to the source increases? Fundamentally, the specific intensity I_ν is conserved along any ray in a vacuum, a universal consequence of energy and phase space conservation (Liouville's Theorem). The telescope's geometry simply reflects this physical law: because the instrumental ratio A_D/f^2 is fixed, the single pixel samples a physically larger area of the source ($A_S \propto r^2$). While the total flux arriving from any specific point on the source drops by $1/r^2$, the telescope pixel is now collecting light from a patch of the source that is exactly r^2 times larger. These effects perfectly cancel out. Therefore, for a **spatially resolved source** (where the source spans multiple pixels), our detector intrinsically measures **Intensity** (often referred to observationally as surface brightness), which remains entirely distance-independent.

However, when observing a **point source** (an *unresolved* source, like a star), we cannot spatially resolve its surface. The entire source fits within a single pixel (or the instrumental seeing disk). We can no longer map a specific source area A_S to a fractional detector area. Instead, we measure the **flux density**, F_ν, obtained by integrating the specific intensity over the solid angle subtended by the source:

$$F_\nu = \int_{\text{source}} I_\nu \cos\theta\, d\Omega \quad [\mathrm{W\ m^{-2}\ Hz^{-1}\ or\ erg\ s^{-1}\ cm^{-2}\ Hz^{-1}}] \tag{26}$$

As geometrically demonstrated in Figure 7, because the integration bounds are fixed over the physical extent of the source, the solid angle subtended by the star physically shrinks as the observer moves further away. Consequently, the measured Flux Density decreases strictly according to the inverse-square law ($1/r^2$). Thus, for a **point source**, we measure **Flux**.

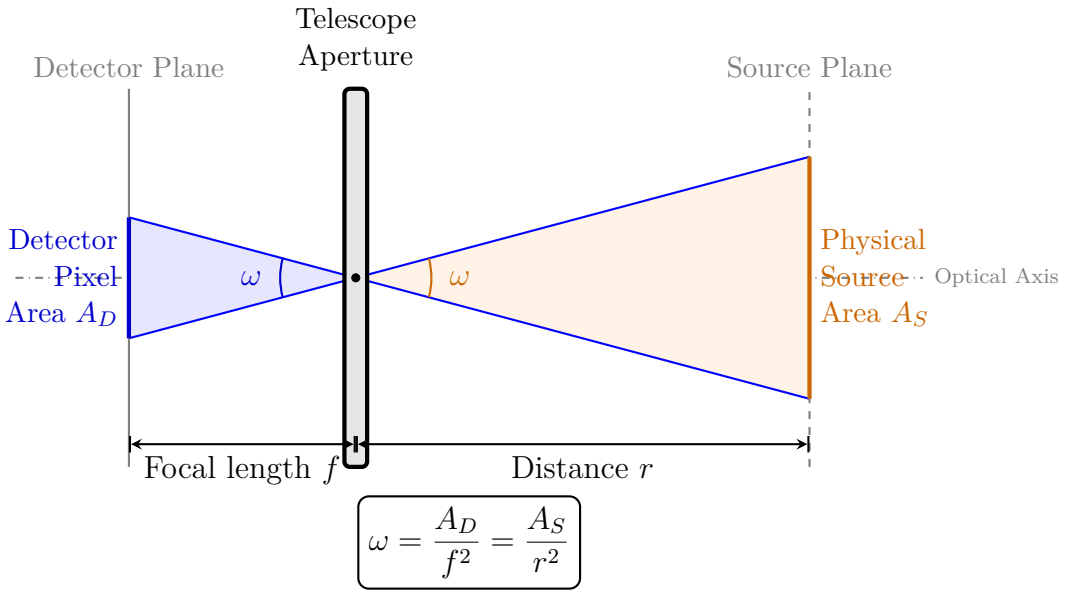

Figure 6: Mapping of a resolved source onto a detector array. Because the rays cross at the optical center, the solid angle ω subtended by a single detector pixel (Area A_D) looking outward exactly equals the solid angle subtended by the mapped source area (A_S) looking inward. If the distance r increases, the pixel simply samples a physically larger area of the source ($A_S \propto r^2$), perfectly canceling out the $1/r^2$ drop in flux and rendering the measured specific intensity distance-independent.

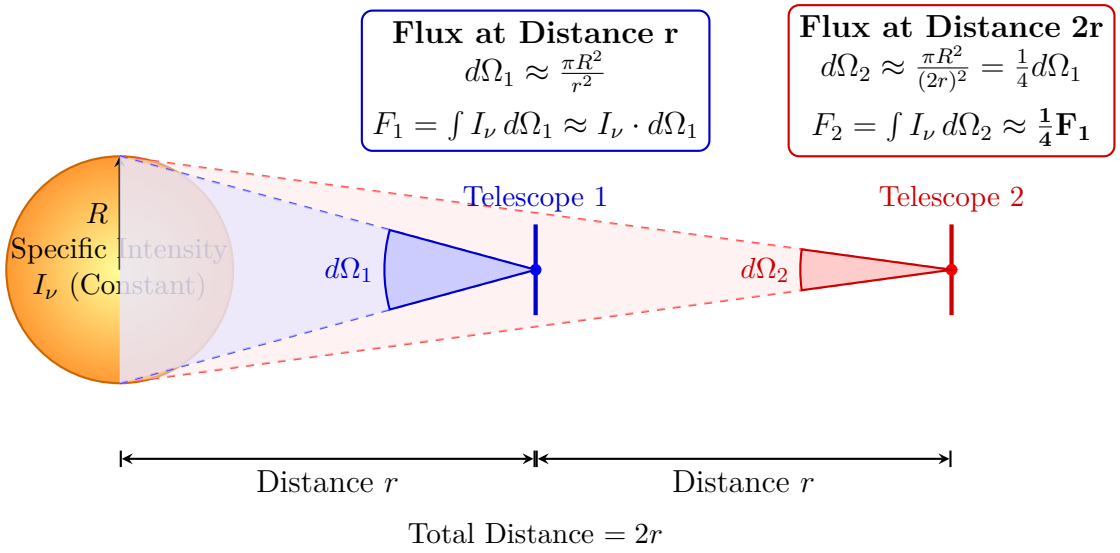

Figure 7: The physical origin of the inverse-square law for unresolved sources. Because the specific intensity (I_ν) emitted by the stellar surface is constant, the measured flux depends entirely on the solid angle ($d\Omega$) the star subtends on the sky. When the distance is doubled from r to $2r$, the integration cone physically shrinks to one-quarter of its area, causing the measured Flux Density (F_ν) to drop by r^{-2}.

5.2 Kirchhoff's Laws and Blackbody Radiation

When observing these fluxes, the resulting spectrum relies entirely on the physical state of the source, summarized by **Kirchhoff's Laws of Radiation**:

1. A hot solid, liquid, or dense gas emits a **continuous spectrum**.
2. A hot, low-density (diffuse) gas emits an **emission line spectrum**.
3. A cool, low-density gas positioned in front of a continuous source produces an **absorption line spectrum**.

The most fundamental example of continuous astrophysical emission is the Blackbody (Corpo Negro). For a perfect continuous emitter, the specific intensity is described mathematically by **Planck's Law**, which depends entirely on the temperature T of the emitting source:

$$B_\nu(T) = \frac{2h\nu^3}{c^2} \frac{1}{e^{h\nu/kT} - 1}$$

Depending on the frequency domain, the Planck function can be approximated by two important analytical limits (as visualized in Figure 8):

- **Rayleigh-Jeans Law ($\frac{h\nu}{kT} \ll 1$):** In the low-frequency limit (such as the radio regime), the exponential term can be expanded via a Taylor series, yielding $B_\nu \approx \frac{2kT\nu^2}{c^2}$.
- **Wien's Approximation ($\frac{h\nu}{kT} \gg 1$):** In the high-frequency limit (such as X-rays or gamma rays), the -1 term in the denominator becomes negligible, yielding $B_\nu \approx \frac{2h\nu^3}{c^2} e^{-h\nu/kT}$.

By taking the derivative of the Planck function with respect to wavelength and setting it to zero, we can find the exact peak of the emission curve. This relationship is known as **Wien's Displacement Law**, which states that the wavelength at which a blackbody emits its maximum specific intensity is inversely proportional to its temperature:

$$\lambda_{max} T = b$$

where $b \approx 2.898 \times 10^{-3}\,\mathrm{m \cdot K}$ is Wien's displacement constant. This fundamental law explains the colors of stars: hotter stars peak at shorter wavelengths and appear blue, while cooler stars peak at longer wavelengths and appear red.

Integrating Planck's law over all frequencies and solid angles yields the total emitted flux (the area under the curve), governed by the **Stefan-Boltzmann Law**:

$$F = \sigma T^4$$

where $\sigma \approx 5.67 \times 10^{-8}\,\mathrm{W\ m^{-2} K^{-4}}$. If we integrate this flux over the entire surface area of a star with radius R, we obtain its absolute luminosity:

$$L = 4\pi R^2 \sigma T^4$$

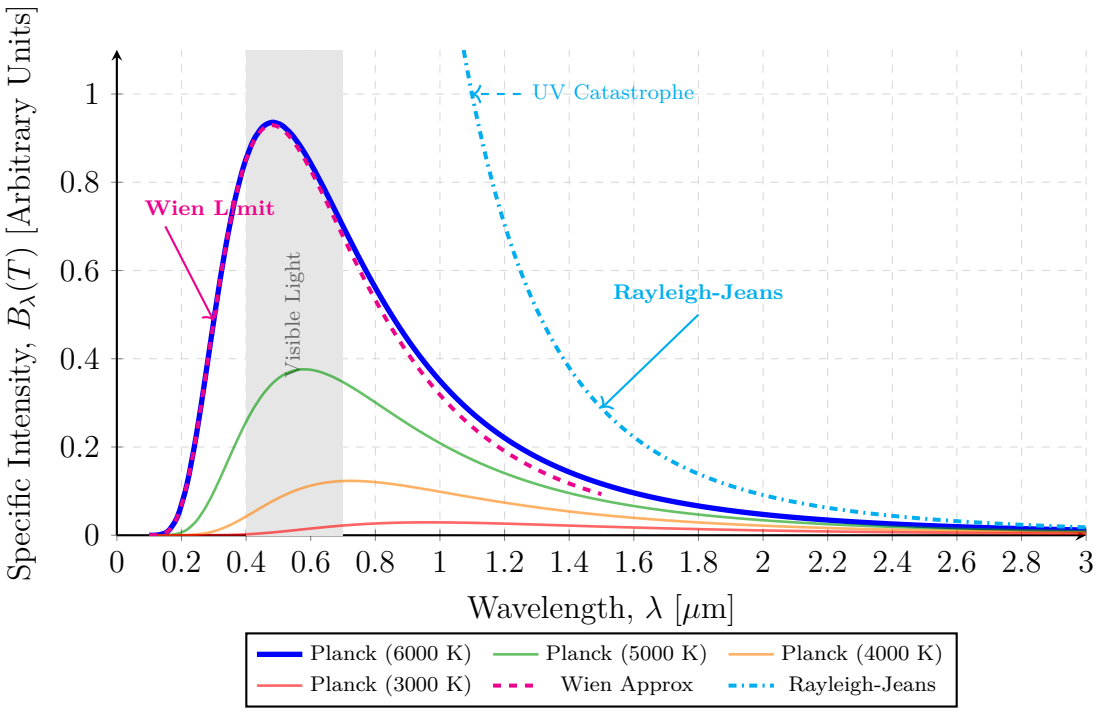

Figure 8: Planck's Law for Blackbody Radiation and its historical limits. The legend is positioned at the base to ensure full visibility within document margins while maintaining a clear view of the Ultraviolet Catastrophe and spectral behavior.

5.3 The F_ν vs. F_λ Trap and SEDs

A common pitfall in multi-wavelength astrophysics arises from the differing conventions of sub-fields: radio astronomers naturally operate in frequency space (F_ν), while optical and UV astronomers traditionally measure flux per unit wavelength (F_λ). While the total energy within a spectral band must be conserved regardless of units ($F_\nu|d\nu| = F_\lambda|d\lambda|$), the inverse relationship between frequency and wavelength ($\nu = c/\lambda$) makes the transformation between these flux densities highly non-linear.

Students often mistakenly equate the two directly, overlooking the necessary chain-rule derivative that steepens the spectrum as one moves across the regime:

$$F_\lambda = F_\nu \left(\frac{c}{\lambda^2} \right) \quad [\text{erg s}^{-1}\ \text{cm}^{-2}\ \text{Å}^{-1}]$$

Because of this $1/\lambda^2$ weighting, a source with a perfectly "flat" spectrum in F_ν will appear to have a steep slope when viewed in F_λ.

This unit-dependent "shifting" of the spectrum becomes dangerous when plotting broad-band Spectral Energy Distributions (SEDs). As shown in Figure 9, plotting an SED using only F_ν or F_λ over several orders of magnitude creates a visual bias: F_ν plots artificially inflate the energetic importance of the radio and infrared, while F_λ aggressively overemphasizes high-energy peaks in the UV or X-ray.

To find where an object truly emits the bulk of its energy, we use νF_ν (or identically, λF_λ).

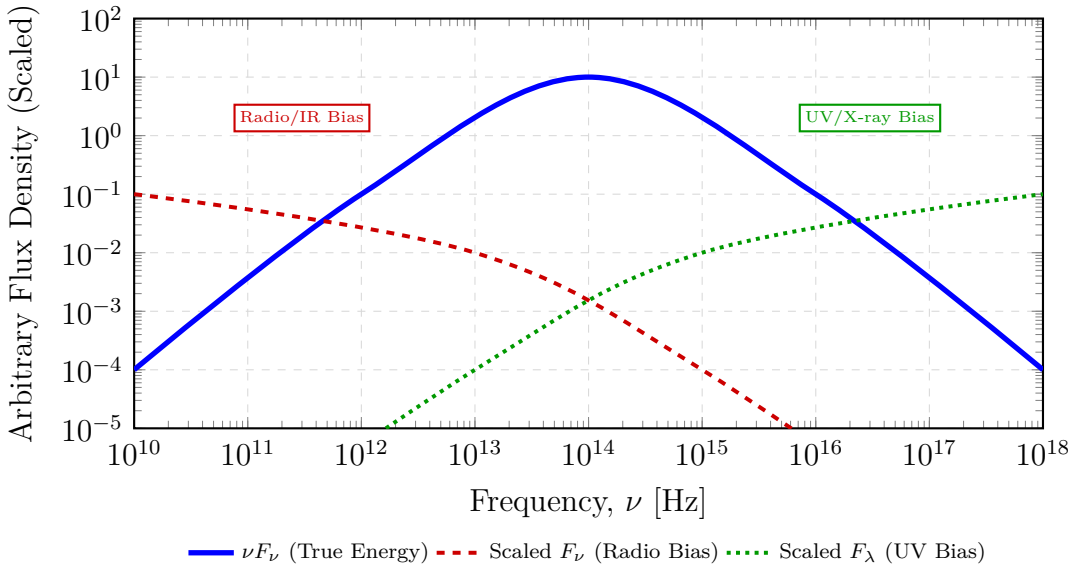

Figure 9: A schematic of the F_ν vs. F_λ trap. When viewed across a broad logarithmic range, F_ν and F_λ shift the "visual peak" of emission. Only νF_ν correctly represents the regime where the bulk of the energy is actually emitted.

The mathematical necessity for this is rooted in the calculation of the total integrated flux (F_{tot}):

$$F_{tot} = \int_0^\infty F_\nu \, d\nu = \int_0^\infty (\nu F_\nu) \frac{d\nu}{\nu} = \int_{-\infty}^\infty (\nu F_\nu) \, d(\ln \nu)$$

Since logarithmic axes ($\log \nu$) are standard for broadband SEDs, the area under the curve only represents the true energetic output if the y-axis is νF_ν. As a final piece of mathematical elegance, this quantity serves as a "unifying language" between sub-fields, as it remains perfectly invariant regardless of whether you measure in frequency or wavelength:

$$\nu F_\nu = \lambda F_\lambda$$

5.4 The Realistic Flux Integral (Energy vs. Photons)

It is critical to remember that modern detectors (like CCDs) are *photon counters*, not *energy meters* (like bolometers). Furthermore, the raw theoretical flux from a star (F_ν^0) is never what reaches the detector array.

The total photon flux N_{tot} measured by a telescope must account for severe environmental and instrumental losses. Over an integration time t and an aperture area A, the measured signal is:

$$N_{tot} = A \cdot t \int_0^\infty \frac{F_\lambda^0(\lambda)}{hc/\lambda} \cdot T(\lambda) \cdot R(\lambda) \cdot S(\lambda) \, d\lambda$$

where:

- $T(\lambda)$: Transmissibility of the Earth's atmosphere.

- $R(\lambda)$: Reflectivity / efficiency of the telescope optics.
- $S(\lambda)$: Transmissibility of the filters and quantum efficiency of the detector.

This layered physical reality underscores why magnitude zero-points are incredibly difficult to anchor perfectly to physical units.

References

[1] Holtzman, J. (2023). *Astronomy 535: Observational Techniques Class Notes*. Department of Astronomy, New Mexico State University.

[2] Hogg, D. W. (2022). *Magnitudes, distance moduli, bolometric corrections, and so much more*. arXiv preprint arXiv:2206.00989v1.

[3] Léna, P., Rouan, D., Lebrun, F., Mignard, F., & Pelat, D. (2012). *Observational Astrophysics* (3rd ed.). Springer.

[4] Chromey, F. R. (2010). *To Measure the Sky: An Introduction to Observational Astronomy*. Cambridge University Press.

[5] Kitchin, C. R. (2020). *Astrophysical Techniques* (7th ed.). CRC Press.

These course notes were refined with the assistance of Gemini 3.1 Pro. Unless otherwise cited, all figures were generated using this tool.
Last updated: April 7, 2026